Hall resistivity in pure cadmium and dilute crystals of *Cd*-Ag and *Cd*-In†‡

D. A. Lilly* and A. N. Gerritsen
Physics Department, Purdue University, West Lafayette, Indiana 47907
(Received 23 July 1973)

The Hall resistivity $\rho_{21}(H,T)$ ($\vec{H}\|[0001]$, $\vec{J}\|[11\bar{2}0]$) has been measured on pure cadmium single crystals and crystals alloyed with In and Ag in the temperature range 1.4–30 K and for field strengths from 1.7 to 24 kG. The residual resistance ratios of the pure samples varied from 16 000 to greater than 30 000; those of the alloys from 62 to approximately 20 000 [corresponding to controlled impurity concentrations from 500 to 1 part per million by weight (ppmw)]. In the pure samples, $\rho_{21}(H,T)$ reversed sign for $T<5$ K, in agreement with previously published results on pure cadmium and a number of Cd-Zn crystal alloys, in which the behavior of $\rho_{21}(H,T)$ for 1.4 K $\leq T \leq$ 10 K was semiquantitatively described in terms of intersheet scattering. In the present alloys, at the lowest temperatures and highest fields, ρ_{21} approaches a positive, constant value even for concentrations of Ag or In as low as 1 ppmw. It is shown that intersheet scattering cannot consistently account for this new behavior. A two-band model, based on published measurements of the temperature dependences of hole and electron mean free paths in cadmium, is found to be only qualitatively successful in describing $\rho_{21}(H, T \leq 10$ K) in the alloys for which ρ_{21} remains positive. It is suggested that combinations of orbital scattering times $\tau(T)$, with various temperature ranges of dominance must be considered for an accurate description of the Hall resistivity in these alloys.

I. INTRODUCTION

Data have been published in an earlier paper[1] on the Hall resistivity $\rho_{21}(H, T)$ of cadmium and dilute *Cd*Zn crystals at low temperatures for H parallel to the hexagonal axis. There the consistent behavior concerning the sign reversal below 4.2 K of the normally positive Hall resistivity was discussed. This behavior was tentatively explained[2] with the assumption of hole-electron transitions at special points on the Fermi surface (FS), between two adjacent sheets formed by the intersection of the second-zone hole surface and the basal (ΓKM) plane. This localized, *intersheet scattering* was considered in combination with the effects of temperature and magnetic field strength; the strong influence of the Zn impurities was incorporated parametrically into a semiquantitative model. Other independent results[3] on dilute cadmium alloys were used to suggest that the intersheet scattering was influenced in a manner characteristic of the solute element.

The present data complete the original data in several respects. First, they include measurements in the temperature range between liquid helium and solid hydrogen, which allows for the determination of the shape and location of the positive maximum in ρ_{21} above the Hall reversal temperature. Secondly, the present results consider the effects of small concentrations of silver and indium, solutes which, unlike zinc, can be expected to produce negligible mass (and, to a lesser extent, size) effects in cadmium. Finally, the data to be reported are for alloys in which the electron per atom ratio $\mathfrak{z}$ was changed with respect to cadmium, as it was not in the *Cd*Zn alloys.

Experimentally, the effect of the presence of impurities on the intersheet scattering was observed to be much larger than was anticipated, even at vanishingly small concentrations. At the few parts per million by weight (ppmw) level, where solute $\mathfrak{z}$ effects on ρ_{21} could no longer be discerned, these solutes nevertheless completely inhibited the intersheet scattering. Finally, the more precise determination of the maximum of $\rho_{21}(T)$ around 5 K made possible a semiquantitative explanation[4] based on observed[5] anisotropic, electron-phonon scattering.

II. EXPERIMENTAL METHOD

A. Sample preparation

Single-crystal samples of pure cadmium and dilute alloys of *Cd*Ag and *Cd*In were prepared from high-grade cadmium (6*N* purity) and high-grade silver and indium (both 5*N* purity). Three pure cadmium samples were cut and planed on a Servomet SMC spark machine from three single-crystals ingots of different origins. Table I presents the impurity analyses of these three samples, their origins, and resistance ratios $r_{4.2\,\mathrm{K}}$. Here r_T = resistance (273 K)/resistance (T).

In general, the crystal growing proceeded along standard lines, with some exceptions. Measured weights of pure cadmium and of the impurity were placed in a quartz ampoule (i.d. 22 mm), which had been drawn to a sharp tip at one end and etched with HF acid and rinsed with distilled water. Since molten cadmium reacts with quartz, a thin insulating layer of carbon was then deposited in the ampoule. This was done by heating the ampoule, which contained a few drops of ethanol, red hot, while turning it slowly on a lathe.

After cooling, the ampoule was rinsed again with

TABLE I. Mass spectrographic analysis[a] of three pure-cadmium samples. (Results in parts per million by weight.)

Sample	Cd No. 1	Cd No. 2	Cd No. 3
Origin	Chemical and Metallurgical Department, Purdue Univ.	Harshaw Chemical Co.	Home made
$r_{4.2\,K}$	30 000	21 300	17 400
Length/width	1.67	2.33	4.93
Thickness (mm)	1.48	2.02	1.97
Element[b]			
B	0.005	0.003	0.002
C	1.	1.	0.5
N	0.2	0.1	0.1
O	3.	3.	3.
F	< 0.05	< 0.05	< 0.05
Na	4.	2.	1.
Mg	0.2	1.	0.05
P	0.03	0.01	0.02
S	0.3	0.2	0.1
Cl	0.6	0.2	0.1
K	0.5	0.3	0.2
Ca	1.	1.	0.7
Ti	0.04	0.04	< 0.02
V	0.02	0.01	0.01
Cr	0.5	0.5	0.3
Mn	c	c	c
Fe	c	c	c
Co	0.05	0.05	0.02
Ni	0.4	0.2	0.2
Cu	0.7	0.7	0.4
Zn	0.4	0.4	0.3
Sr	0.07	0.01	0.007
Zr	0.4	0.2	0.1
Nb	0.02	0.02	0.01
Ag	< 0.2	0.2	< 0.2
Cd	major	major	major
In	< 0.1	< 0.1	< 0.1
Sn	3.	< 1.	< 0.5
Ta	< 6.	< 6.	< 6.
Hg	< 0.06	10.	0.2
Pb	0.1	0.2	0.1

[a]Analysis by Battelle Memorial Institute.
[b]Elements not listed are not detected and less than 0.3 ppmw.
[c]Cd interference.

distilled water to remove carbon flakes and dried. The filled ampoule was then pumped down to less than 2×10^{-5} Torr and sealed off with a torch. To insure complete outgassing pumping was continued until the pressure did not exceed this value while gentle heat was applied to the ampoule with a torch. The sealed ampoule was placed in a vertical holder in a Bridgman furnace. After the temperature at the ampoule site (as measured by a Pt-Pt + 13%-Rh thermocouple) was maintained at 340 °C for approximately 24 h, the oven was raised at a rate of 4.8 mm/h. The proper growth rate was determined by trial and error, and is ten times slower in the present instance than the rate reported elsewhere[6] for the growth of 4-mm-diam single-crystal rods. The need for this lower rate may be attributed to the large diameter of the rods (22 mm) and the actual temperature profile of the furnace. The crystals grown in this manner were 7 or 8 cm long, pointed at one end, where growth began. Within a few degrees, crystal orientation was found to be one of two types: the hexagonal axis parallel or perpendicular to the growth axis.

*Cd*In *alloy crystals.* The *Cd*In alloys were produced by two methods. Two samples were prepared by diffusing indium into a slab of single-crystal cadmium; the others were grown as single crystals from a melt of cadmium and a controlled amount of indium. The total indium content in samples produced by both methods varied between 5 and 400 ppm. Table II presents the results of impurity analyses of all *Cd*In samples, along with the resistance ratios ($r_{4.2\,K}$) and the method of preparation.

In the diffusion method, a wafer-shaped piece of single-crystal cadmium was plated on both sides with indium. The plating was done with a clean solder iron, the tip of which was cleaned and rinsed first in nitric acid and then in distilled water, then plated also with indium. The plated wafer was then annealed for several days at 200 °C in a helium atmosphere, after which the layers of indium were removed by spark planing both sides of the wafer. A sample in the shape of a rectangular solid was then cut from the wafer, etched in a dilute solution of HNO_3 and ethanol (to remove spark damage and surface impurities), and annealed in a helium atmosphere at 200 °C for several more days. The purpose of the final anneal was twofold: (i) to remove strains in the sample introduced during handling, (ii) to homogenize the impurities. Evidence exists that room-temperature annealing (for several weeks) is sufficient to remove strains, as is annealing at 100 °C for one day.[7] The extent of homogenizing due to annealing can only be inferred.

A test for homogeneity of one *Cd*In sample that was prepared by diffusion was made by measuring the resistance ratio $r_{4.2\,K}$ after the sample thickness was reduced. Between measurements, the solder, which contained indium, was removed by spark cutting. The sample was cleaned and its thickness reduced by etching. Then the sample was annealed as described above. By this process, the sample thickness was reduced by a factor of 2, at least. Table III presents the results of this test. The final 8% variation in $r_{4.2\,K}$ compares well with that encountered in similar tests on some *Cd*Zn alloys[8] and is indicative of reasonably good sample homogeneity.

Four additional *Cd*In samples were prepared from single-crystal ingots, which were grown from

TABLE II. Impurity analysis[a] of *Cd*-In alloys, prepared by solute diffusion (*D*) and grown from melt (*M*) (in parts per million by weight).

Sample	$r_{4.2K}$	Length/Width	Thickness (mm)	In (OES)[b]	In (SSM)[c]	Sn	Cu	Hg
Cd-In-*C* (*D*)	195	2.66	0.59	200	•••	10	not detected	•••
Cd-In-3 (*M*)	833	5.22	1.89	50	50	not detected	not detected	•••
Cd-In-*B* (*D*)	3560	2.26	0.99	10	•••	not detected	not detected	•••
Cd-In-*HG2* (*M*)	19500	5.44	2.00	< 5	0.4[d]	not detected	not detected	1
Cd-In-4 (*M*)	16800	4.58	2.01	< 5	2.0[d]	not detected	not detected	0.2

[a]Analysis by Battelle Memorial Institute
[b]Analysis by optical-emission spectrography.
[c]Analysis by spark-source mass spectrography
[d]Accuracy ± 3 times stated value.

the melt *in vacuo* by the Bridgman method. The low solubility of indium in cadmium in this phase[9] (< 1.4 at.%) made the crystal growing difficult, but the problems were found to be manageable.

*Cd*Ag *alloys*. These alloys were all made by the Bridgman method described above. The silver content in these alloys varied between 1 and 500 ppm. Table IV presents the impurity analyses of these samples along with their resistance ratios at 4.2 K. The rather large limits set for the impurities other than silver are artifacts of the emission spectrographic analysis, and are better represented by the impurity content of the pure samples for the same elements as given in Table I.

The low solubility of silver in cadmium[10] (< 3.1 at.% at 100 °C) did not present as great a problem in growing these crystals as did the difference of 640 °C between the melting points of the components. The following method was finally established: the cadmium was held at 340 °C, 20 °C above its melting temperature; the silver was allowed to diffuse into the molten cadmium. After about three days at the same temperature, the Bridgman furnace was raised. During the latter hours of growth, the oven itself provided a first anneal for the new crystal.

To obtain some information about the impurity gradient on a macroscopic scale in one of the *Cd*Ag ingots, the resistance ratios ($r_{4.2\ K}$) of two samples, taken from cross sections 50 mm apart from the top and bottom of the ingot, were measured. These ratios were found to be 1526 and 1829, respectively. The smaller ratio was obtained from the sample cut from the top of the ingot, where impurities would be expected to migrate during crystal growth. The 20% difference in $r_{4.2\ K}$ over 50 mm, as measured above, when taken to represent the impurity gradient over the same distance, would result in a gradient of less than 1% over 1 or 2 mm, the thickness of a typical sample. To further insure homogeneity and nearly identical sample histories, however, the *Cd*Ag samples were also annealed at 200 °C in a helium atmosphere for several days.

Samples Cd-Ag-*B*, Cd-Ag-*C*, Cd-Ag-*D* were obtained by successively diluting *Cd*Ag ingots by a factor of 2. The initial ingot had a resistance ratio equal to 1500, and an estimated Ag concentration of 0.006 at.%. Successive dilutions produced ingots from which samples of resistance ratios ($r_{4.2\ K}$) of 2460, 5030, and 7050 were taken. Table IV shows that while $r_{4.2\ K}$ increases as expected with decreasing silver content, there is poor quantitative correspondence between $r_{4.2\ K}$ and the silver concentration, in contrast to the good correspondence evident in the *Cd*In samples (Table II). This suggests that variations of the silver concentration on a microscopic level may be playing an important role. Indeed, the silver concentration in these samples was found during analysis to be nonuniform, varying locally by a factor of 3 in one sample, Cd-Ag-*E*, but, more commonly by (25–50)%. The inconsistent behavior of the Hall resistivity observed in sample Cd-Ag-*E* may be due to such a variation, and these results have therefore been excluded from discussion. To provide an accurate estimate of the silver concentration, a sampling technique was devised to arrive at an average (representative) value, and this average is presented in Table IV. This number is probably a good estimate of the macroscopic silver content, to which the resistance ratio is evidently sensitive (see above). It may overestimate the microscopic silver density, to which, at these low concentrations, the magnetotransport phenomena may be very sensitive. The combination of the $r_{4.2\ K}$ value and the analysis confirm that Cd-Ag-9 is the sample with the lowest silver concentration.

B. Sample holder and cryostat

The samples were cut from the ingots after these had been oriented by standard x-ray techniques to

TABLE III. Results of homogeneity test for one *Cd*In sample.

Sample	Thickness (mm)	Anneal	$r_{4.2K}$
*Cd*In	~1	no	4000
	~0.75	7 days at 200 °C	5000
	~0.5	7 days at 200 °C	5400

TABLE IV. Impurity analysis[a] of *Cd*Ag alloys. (Results in parts per million by weight).

Sample	$r_{4.2\,K}$	Length/Width	Thickness (mm)	Ag	In	Bi	Sn	Pb	Cu	Fe
Cd-Ag-1	68	7.88	1.03	500[b]	500[c]	100[c]	1000[c]	100[c]	200[c]	2[c]
Cd-Ag-*B*	2460	5.84	0.80	25	< 3[d]	< 3[d]	< 3[d]	< 3[d]	< 1[d]	< 1[d]
Cd-Ag-*E*	2810	4.80	2.35	2	↓	↓	↓	↓	< 1	↓
Cd-Ag-*C*	5030	5.02	1.58	8	↓	↓	↓	↓	1	↓
Cd-Ag-*D*	7050	5.23	2.00	7	↓	↓	↓	↓	1	↓
Cd-Ag-9	12500	4.99	1.59	1	↓	↓	↓	↓	< 1	↓

[a]Analysis by Battelle Memorial Institute.

[b]This value obtained by atomic absorption. The remaining Ag and all impurity data were obtained by optical-emission spectrography.

[c]Contents vary by ± 3*X*. Large non-silver impurity content for sample Cd-Ag-1 is due to the incomplete removal of Cerroseal solder, present at the sample surface only.

[d]These elements were not found at these detection limits.

within 0.1° with respect to the desired crystal plane. A recheck of several samples in their final form revealed that the orientation, with careful handling, could be preserved within ±0.5°. The samples were cut into a standard shape with a spark-cutting die that cut four small potential arms on the rectangular solid form. The diffusion-prepared samples (Cd-In-*C*, Cd-In-*B*) were too small for the die, and were cut into rectangular solid forms. Potential leads were soldered onto the arms of the samples [(arm length)/(arm width) ≥ 10] or to solder dots placed on the smaller samples with Cerroseal-35 solder. Sample dimensions were measured after completing all resistance measurements. Hall voltages odd only in H were determined from the appropriate average of the four voltages obtained from field and current reversals.

The samples were mounted on a stainless-steel holder which was lowered into the tail section of a commercial, intermediate-temperature cryostat (Sulfrian Select-a-Stat No. 965). The tail section was placed between the pole pieces of an electromagnet, providing field strengths up to 25 kG. By rotating the sample in the field and observing the sharp minimum in the magnetoresistance for $\vec{H} \parallel [10\bar{1}0]$, the adjustment of $\vec{H} \parallel [0001]$ was possible[11] to within 1°.

The temperature (T) of the sample was varied between 1.4 and 100 K, and measurements were taken at selected fixed temperatures. In the range $4.2 < T < 100$ K the sample environment was heated with a manganin wire heater while, simultaneously, the area around the sample was cooled with cold helium gas. The gas was introduced by forcing liquid helium through a long copper capillary to a diffuser located directly beneath the sample. The liquid helium vaporized after passing through the diffuser, thus providing the sample chamber with a cold gas ($T > 4.2$ K). By opening the throttle value completely, with 6–8-cm overpressure, one could flood the sample chamber with liquid helium, to achieve operation between 1.4 and 4.2 K.

The sample was placed inside a copper can which served to protect it from direct gas flow which could produce large temperature instabilities. A 20-Ω length of No. 36 manganin wire (the heater referred to above) was wound around the can and secured to it with a light coating of GE 7031 varnish. Current was supplied to the heater by an Artronix 5031 proportional temperature controller, for which an Allen-Bradley $\frac{1}{8}$-W 100-Ω nominal resistance carbon resistor, thermally mounted in an aluminum block, served as a temperature sensor. This carbon resistor was observed to have a magnetoresistance ratio $\Delta R/R_0$ small enough to avoid instabilities in the feedback system of the controller (and hence, the temperature set point) when the magnetic field was applied. $\Delta R/R_0$ can be estimated from the Clement-Quinell interpolation formula[12] for the magnetoresistance of 1-W Allen-Bradley resistors to be 0.2%. This agrees well with the maximum $\Delta R/R_0 < 0.1\%$, that could be tolerated as computed from the typical Artronix sensitivity (1 mK) and the zero-field resistance[13] formula for the resistor used. With this setup, short-range temperature stability was typically a few mK, but temperature drifts of 20 mK for $4.2 < T < 10$ K and 10 mK for $T > 10$ K were common during a measurement run which lasted approximately $\frac{1}{2}$ h. For measurements below 4.2 K, in which case the temperature was controlled by vapor pressure regulation, the stabilization was better than 0.01 K.

C. Voltage measurements

Sample voltages. Sample currents up to 3 A (stability ±0.01%) were provided by a regulated power supply (NJE Model EB 18-3M). The sample voltages were measured with a Keithley 148 (K148) nanovoltmeter (resolution better than 10^{-9} V) in combination with a Keithley 260 (K260) nanovolt source, which was used for calibration purposes

and for bucking out small thermal voltages (typically a few tenths of a microvolt). In order to increase measuring sensitivity under normal experimental conditions, the 1-V full-scale output of the K148 was averaged in a six-digit integrating voltmeter (DVM). By varying the integration time of this device, it was possible to achieve $\frac{1}{2}$-nV sensitivity, and day-to-day reproducibility in the nanovolt range of 10%.

The accuracy of the absolute voltage measurements was limited only by the accuracy of the full-scale output of the K148, which was found to be 1 V (±0.1%) or better for all ranges used. This was determined by the DVM, which was first calibrated with a laboratory standard cell (Weston No. 24351). An independent check of the DVM calibration was made by measuring a 1-V output of the K260 (calibrated against a Leeds and Northrup 8687 potentiometer, accuracy ±0.03%). Afterwards, voltages detected by the K148 could be read directly from the DVM, to within ±0.1% ±$\frac{1}{2}$ nV, or better.

Temperature determination. The temperature was determined by comparing the measured resistance of a calibrated germanium sensor (Cryocal No. 1486) with interpolation tables supplied by the manufacturer. Stable currents (stability better than 0.05%) of 1 or 10 μA were supplied by telephone relay batteries to the sensor, which was thermally connected to a stainless-steel sample platform, directly opposite the sample. Temperature resolution was 1 mK, but owing to drift, could be determined absolutely only to ±0.01 K.

Estimation of errors. For a judgment of the reliability of the data obtained, an estimate of the measurement precision is necessary and has to be seen in connection with the sources of error due to the sample's construction. The calculation of the relative uncertainty in a single measurement is simple and straightforward.[14]

The Hall resistivity is given by $\rho_{21} = V_H t/I$ (where V_H is the Hall voltage, t is the sample thickness, and I is the sample current). The relative uncertainty in ρ_{21} for V_H in the range encountered (50–500 nV) follows as $1.8\% \leq \Delta\rho_{21}/\rho_{21} \leq 5.4\%$ for estimates of $\Delta I/I \approx 0.01\%$ and $\Delta t/t \approx 1\%$. The lower percentage refers to high-field measurements, the higher percentage to low-field data results obtained at higher temperatures. The uncertainty $\Delta\rho_{11}/\rho_{11}$ in the sample resistance is controlled by the resolution of the nanovoltmeter and is estimated to be $\Delta\rho_{11}/\rho_{11} \leq 0.01\% \pm 0.2\% \pm 1/V_{11}$, V_{11}(nV) for two current directions $\pm I$. For $H = 0$ this results in an uncertainty in R of 10% for a 10-nV sample voltage, a typical voltage of the purest samples at the lowest temperatures. The experimental quantity of interest $r_T = R_{273\ K}/R_T$, propagates essentially only the uncertainty in R_T, since $(\Delta R/R)_{273\ K} \leq 0.2\%$, and r_T is independent of sample dimensions (neglecting lattice contraction effects, which can be estimated from thermal expansion data[15] to be of the order of 1%). The magnetic field was calibrated with a Rawson coil gaussmeter (probe 16290, type 720), accurate to approximately 1%.

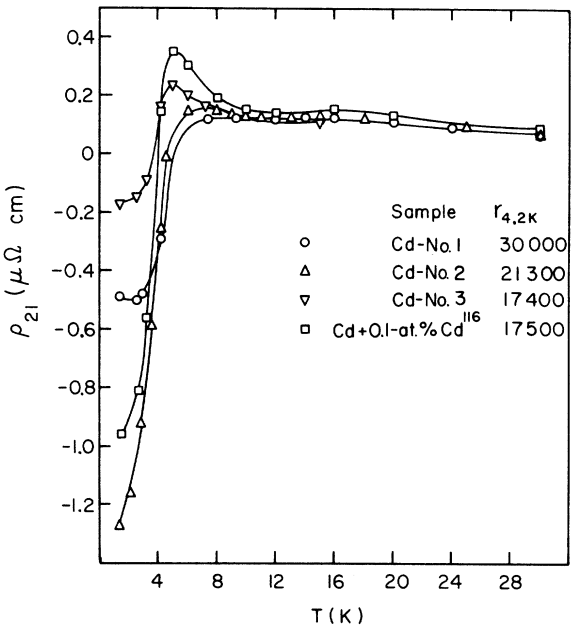

FIG. 1. Hall resistivity ρ_{21} ($H = 20$ kG, T) against T for the pure samples and sample Cd-Cd^{116}.

III. RESULTS

A. Pure cadmium

The results of ρ_{21} ($H = 20$ kG, T) for the pure-cadmium samples, along with data obtained on a sample prepared from 6N cadmium and 0.1-at.% Cd^{116} (see Sec. III B for justification for the inclusion of this sample) are presented in Fig. 1. In all cases ρ_{21} reverses sign below 5 K. These results confirm data reported elsewhere.[1,3] However, with the larger number of samples investigated, it is observed that the magnitude of ρ_{21} in the negative region varies rather markedly from one sample to another. Such variations are unexpected, considering that the sample handling histories, resistance ratios, and impurity analyses are nearly identical. The causes of the variations are, however, insufficient to destroy the essential low-temperature character of $\rho_{21}(T)$, that is, the sign reversal. Above $T = 10$ K, the behavior of $\rho_{21}(T)$ is identical for all samples: $\rho_{21}(T)$ increases to a maximum around 15 K, and then decreases continuously for increasing T. Between 4.2 and 10 K, $\rho_{21}(T)$ may or may not exhibit a maximum, which appears at approximately 5 K. It should be noted that the sample that does not exhibit such a maximum also has the highest Hall reversal temperature.

In this temperature interval (4.2–10 K) it can be argued from the data that the normal behavior of $\rho_{21}(T)$ in cadmium is to increase below 10 K. This increase is observed in the alloys as well and will be discussed in Sec. IV B. If the intersheet scattering mechanism responsible for the Hall reversal is sufficiently strong, the increase in $\rho_{21}(T)$ below 10 K cannot occur, and sign reversal occurs at some "high" temperature (5 K in the data). The sign reversal of ρ_{21} at lower temperatures for the other samples indicates that here a relatively weaker intersheet scattering is operating; for these samples, the maximum in $\rho_{21}(T)$ has already been established.

With an aim at studying the effect on ρ_{21} from impurities that changed the mass (with respect to the solvent) without also changing ϑ, sample Cd-Cd^{116} was prepared (see Sec. III B). The small amount of stable isotope added in this sample produced mass changes comparable to or greater than those produced by the *Cd*In and *Cd*Ag alloys in which ϑ and mass were changed simultaneously. From Fig. 1 it can be seen that the behavior of $\rho_{21}(T)$ for the Cd-Cd^{116} sample is fundamentally the same as that for pure Cd.

One might speculate as to why the magnitude of ρ_{21} for temperatures below the Hall reversal differ so widely for three samples of similar handling histories, each of which is presumed to be pure cadmium on the basis of spectrographic analysis and resistance ratio. Examination of the sample surfaces by x rays during crystallographic orientation revealed no irregularities in structure. However, irregularities not detected by these methods could be present in sufficient densities or at particular locations which could affect the intersheet scattering and thereby the Hall resistivity. These irregularities could be in the form of vacancies, twin or slip planes (or both), and stacking faults, all or none of which could be impurity associated. At any rate, the data show that the over-all character of the Hall resistivity in pure cadmium (e.g., sign reversal) is insensitive to the microscopic variations described above. Quantitatively such variations can have a relatively large influence. The results with the dilute alloys clearly demonstrate this feature.

B. Cadmium alloys

In Fig. 2 the results are given for ρ_{21} ($H = 23$ kG, T) for representative *Cd*Ag and *Cd*In samples ($\vec{H} \parallel [0001]$, $\vec{J} \parallel [11\bar{2}0]$). Details of the field dependence of ρ_{21} are given in Fig. 3 for four samples. Above 10 K, the results agree with those of pure cadmium; ρ_{21} attains a maximum near $T = 15$ K, and then decreases for increasing temperature. Below this 15 K maximum there is a slight decrease followed by a rise that is steeper and of greater magnitude for the pure samples, in turn followed by a sharp decrease down to temperature-independent values. These residual values are positive and increase with decreasing sample impurity. For sample Cd-In-4, $\rho_{21}(T)$ exhibits below 4.2 K the sign-reversal characteristic of the behavior in pure cadmium. No qualitative effect of ϑ can be seen.

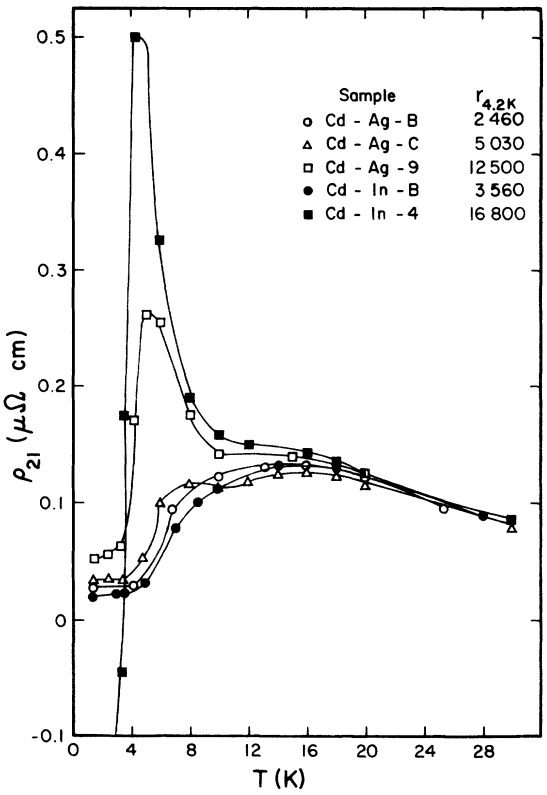

FIG. 2. Temperature dependence of ρ_{21} ($H = 23$ kG, T) for representative *Cd*Ag and *Cd*In samples.

In an attempt to find an indication for the cause of the inhibition of the sign reversal by such extremely small amounts of Ag or In, a crystal was made in which the composition of Cd^{116} was nominally enhanced by 0.1%. Since the natural abundance of Cd^{116} in the metal is 7.6%, any behavior different from the other pure-Cd samples would be unexpected. However, this sample could indicate an eventual effect of mass changes that are larger than those connected with a few ppm Ag and In.

Unfortunately, it was not possible to detect the exact amount of Cd^{116} present in sample Cd-Cd^{116}. This would have been desirable in order to establish quantitatively the mass change produced. However, in view of the drastic changes in ρ_{21} resulting from only a few ppm indium or silver in cadmium, the addition of only 10–100-ppm Cd^{116} in this sample is a sufficient level for testing the mass-change effect on ρ_{21}. This reduced level was in all probability attained. Apart from an ob-

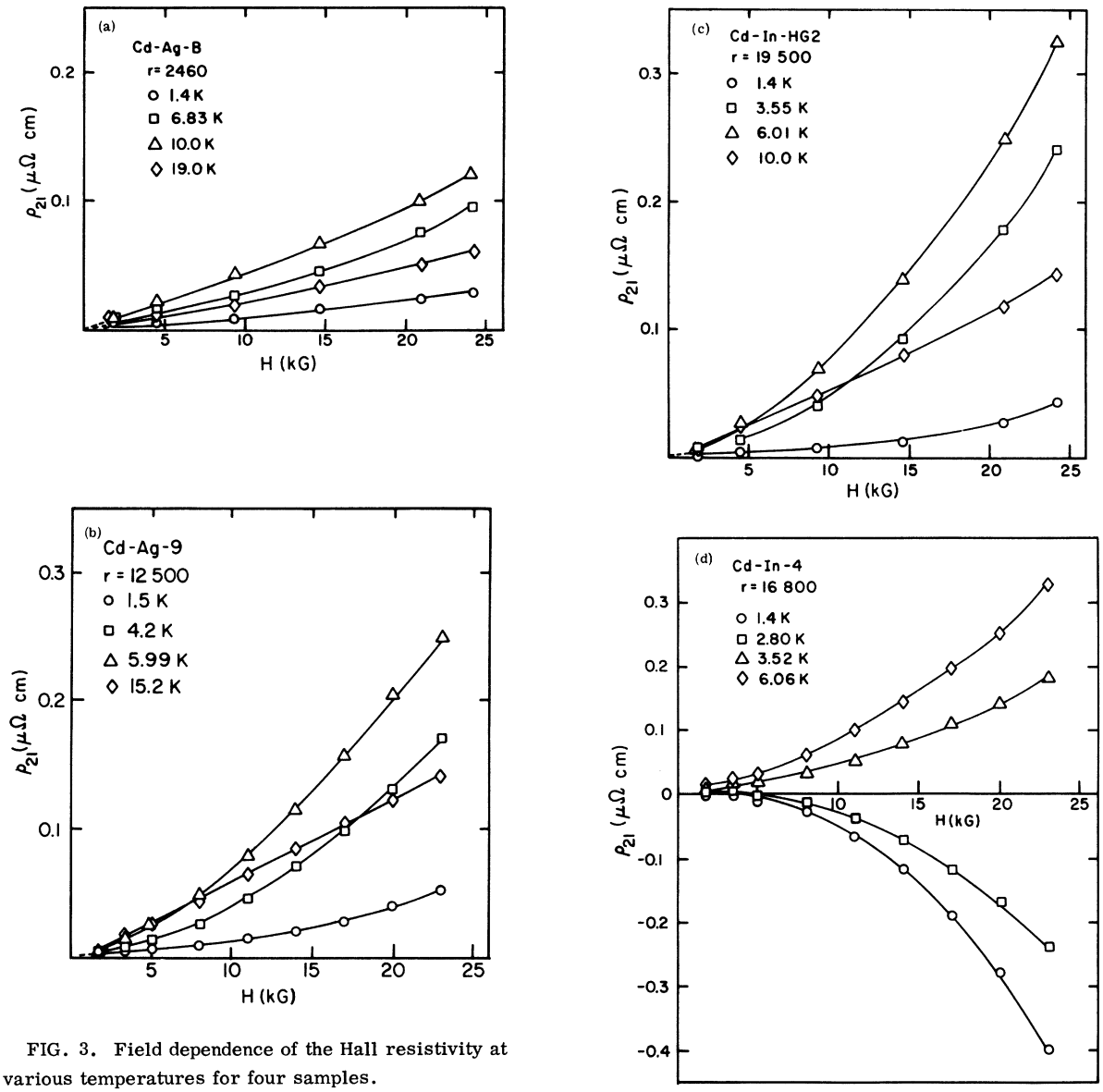

FIG. 3. Field dependence of the Hall resistivity at various temperatures for four samples.

served increase in the magnitude of ρ_{21} (max) the data for this sample (Fig. 1) are comparable to those for the pure-Cd crystals.

The sign reversal of the Hall resistivity is a clear demonstration[2] of the lack of a uniform consistent relation between ρ_{21} and the product $\omega\tau$. It is worthwhile to reinvestigate the possible existence of a Kohler-type behavior in the present case when sign reversal is not observed. The existence of a more or less normal behavior for temperatures above the low-temperature maximum could be at least encouraging.

Figure 4 is a Kohler diagram of the Hall resistivity for representative *Cd*Ag and *Cd*In samples. If Kohler's rule is obeyed, the ordinate in Fig. 4, which is the experimental ratio $\rho_{21}(H, T)/\rho_{11}(0, T)$, will be a function only of $\omega\tau \propto r_T H$. In cadmium $r_T H = 10^4$ kG corresponds[1] to a free-electron $(\omega\tau)_f$ value of 3.6. The line drawn through the symbols, which indicate the respective ordinates for the different alloys, is a representation of the data for a pure-cadmium sample (Cd No. 3). Deviations from Kohler's rule occur over the entire range of $r_T H$, exceeding two orders of magnitude at the largest value of $r_T H$. However, if the data for $T \lesssim 9$ K are momentarily ignored, it can be seen that the remaining data lie within a band which is roughly parallel to the line drawn of slope equal 1. These data display the field dependence of ρ_{21} expected from a compensated metal, and they obey Kohler's rule within the width of the band (roughly, a factor of 2 in the ordinate). This certainly does not represent a

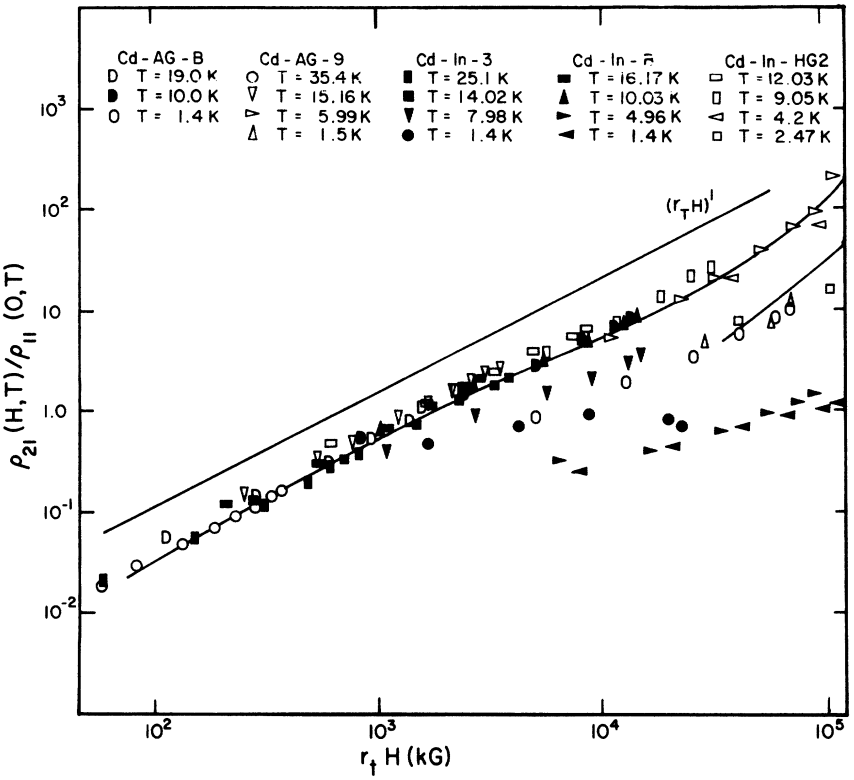

FIG. 4. Kohler diagram of the Hall resistivity for representative samples. The solid line through the data points connects data for the pure sample Cd No. 3.

strict adherence to Kohler's rule.

Much larger deviations from Kohler's rule are evident from Fig. 4 for the data for $T \lesssim 9$ K. The typical field dependence of $\rho_{21}(H, T)$ in this range is linear for small H (usually less than 10 kG), and approximately H^3 for large H. Note that the deviations from Kohler's rule persist in these data for the lowest fields measured (1.72 kG), well within the field range where at higher temperatures $\rho_{21} \propto H$. In Sec. IV A the behavior of ρ_{21} below the low-temperature maximum will be considered in connection with intersheet scattering.

IV. DISCUSSION

A. Intersheet scattering

The sign reversal of ρ_{21} observed in sample Cd-In-4 (Fig. 2) suggests that in the present alloys the general formal conditions[2] for large effects from intersheet scattering are met ($\omega\tau \geq 1$). Hall-resistivity behavior similar to that shown by the *Cd*Zn alloys is expected to be observed. From the choice of the parameter τ used for the *Cd*Zn data,[2] it could be deduced that τ increased with decreasing impurity concentration. This kind of dependence

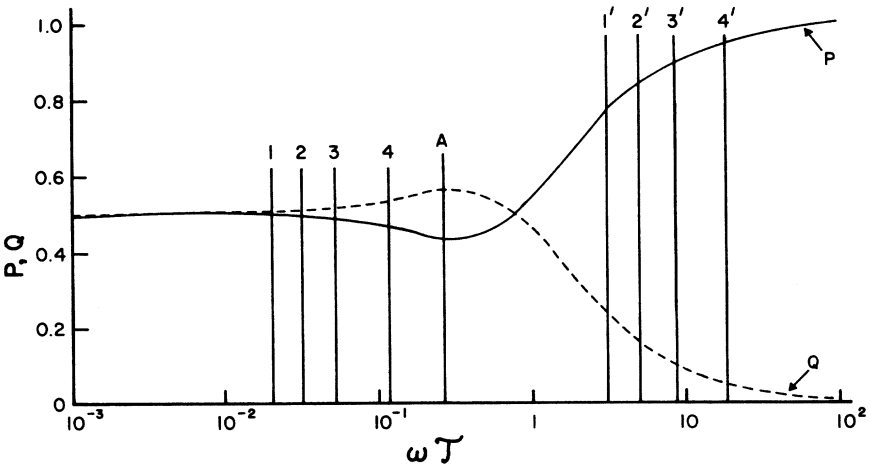

FIG. 5. Variation of P and Q as a function of $\omega\tau$ ($\omega \propto$ field strength, τ = intersheet scattering parameter). Q is the probability for a hole orbit on the clover-leaf tip in the basal plane to transfer to an electron orbit, and $P = 1 - Q$ (taken from Ref. 2, with vertical lines added).

was consistent with the observed impurity-enhanced intersheet scattering. The effect of intersheet scattering was evident even for temperatures as high as 10 K, but is of special interest for comparative reasons in the residual temperature range only, where ρ_{21} no longer changes with temperatures. In the *Cd*Zn alloys the residual values of $\rho_{21}(0)$ decrease with decreasing impurity concentrations, more or less approaching the behavior of pure cadmium continuously. This is in marked contrast to the behavior of ρ_{21} in the present alloys (Fig. 2), where $\rho_{21}(0)$ increases with decreasing impurity concentration, returning to pure-cadmium behavior in a very small impurity range. It will be shown that this behavior is not compatible with the intersheet scattering phenomenon.

Figure 5 is a plot of P, Q vs $\omega\mathcal{T}$ taken from Ref. 2. Here Q is the probability that a hole on the second-zone clover-leaf tip of the cadmium hole surface undergoes intersheet scattering, and $P = 1 - Q$. Let the vertical lines represent values for various samples in the residual temperature range. Let line A represent the $\omega\mathcal{T}$ value of pure cadmium, when $\rho_{21} < 0$: then in terms of this theory both conditions $\omega\tau > 1$, $\omega\mathcal{T} \leq 1$ are satisfied. Lines 1–4 are arbitrary $\omega\mathcal{T}$ values for cadmium alloys, drawn only consistently with the proviso that $\omega\mathcal{T}$ (concentration 1) < $\omega\mathcal{T}$ (concentration 2) when (concentration 1) > (concentration 2), and similarly for the combination 2-3 and 3-4. The positions of lines 1–4 illustrate that, with decreasing impurity concentration, $\rho_{21}(0)$, as in the case of *Cd*Zn alloys, decreases and continuously approaches the value of ρ_{21} for the pure sample. Clearly the behavior of $\rho_{21}(0)$ in the present results is not described by this picture (lines 1-4).

However, one way to account for consistent positive values of $\rho_{21}(0)$ in the present alloys is to shift lines 1–4 to the right of line A (lines $1'$–$4'$), assuming again that $\mathcal{T}$ increases with decreasing impurity concentration. Let line $1'$ intercept the P, Q curves such that $\rho_{21}(0) > 0$. Then Fig. 5 predicts that $\rho_{21}(0)$ will become increasingly positive with decreasing impurity concentration, as the present data indicate.

Fitting samples Cd-In-4 and Cd-In-*HG*2 into this picture is then difficult. For Cd-In-4, $\rho_{21}(1.4\ \mathrm{K}) < 0$, $r_{1.4\ \mathrm{K}} \approx 1.5 \times 10^4$ and the sample's over-all Hall behavior is similar to that of pure cadmium. Thus its $\omega\mathcal{T}$ value will lie close to that given by the position of line A in Fig. 5. But for Cd-In-*HG*2, $\rho_{21}(1.4\ \mathrm{K}) > 0$, $r_{1.4\ \mathrm{K}} \approx 1.7 \times 10^4$ and its $\omega\mathcal{T}$ value must lie close to line $4'$, in order to achieve behavior of $\rho_{21}(0)$ consistent with the rest of the alloys. It is difficult to account for such discontinuous behavior in $\mathcal{T}$ in these two samples, which differ in indium concentration by only 1 or 2 ppm. One must account for a jump in $\mathcal{T}$ in the direction A to $4'$ in Fig. 5 by impurity concentrations of the order of 1 ppm, and the recovery of *pure*-cadmium behavior via *increasing* impurities. Such behavior is physically unreasonable.

Complicating this picture even more is the field dependence of $\rho_{21}(0)$ for two impure samples, Cd-In-*C* and Cd-Ag-1. The field dependence shows ρ_{21} behavior more consistent with $\omega\mathcal{T}$ values near position 1 and $1'$. For these samples $\rho_{21}(0)$ is not increasing at the highest fields (as it would for $\omega\mathcal{T}$ at $1'$), but is bending over, in a pattern characteristic of the *Cd*Zn alloys (see Fig. 6). Therefore, in terms of Fig. 5, another picture of intersheet scattering emerges for the present alloys: the higher-concentration alloys have $\omega\mathcal{T}$ values in the 1–4 range, and the lower-concentration alloys in the $1'$–$4'$ range. This suggests that a few ppm impurities increase $\mathcal{T}$, and a few hundred ppm impurities decrease $\mathcal{T}$. There remains, however, no continuous approach to line A (and pure-cadmium behavior) in Fig. 5 either from the left (decreasing impurity concentration) or from the right (increasing impurity concentration). Again, this explanation seems to be physically unreasonable.

Alternatively, one could suggest that a decreasing concentration of Ag or In in cadmium may act to decrease the intersheet scattering time (the inverse of the *Cd*Zn case). In terms of Fig. 5, only $\omega\mathcal{T}$ values to the left of line A for this case will account for consistent $\rho_{21}(0)$ behavior. However, with this suggestion, the discontinuous approach to the negative value of ρ_{21} for pure cadmium is still more pronounced. At the same time, the notion of an impurity-enhanced intersheet scattering would evidently have to be abandoned.

Finally, within the intersheet-scattering formalism, ρ_{21} will remain positive if $\omega\mathcal{T} \geq \omega\tau$, i.e., $\mathcal{T} \geq \tau$. It is difficult to see how this particular constraint could be maintained. As has been argued,

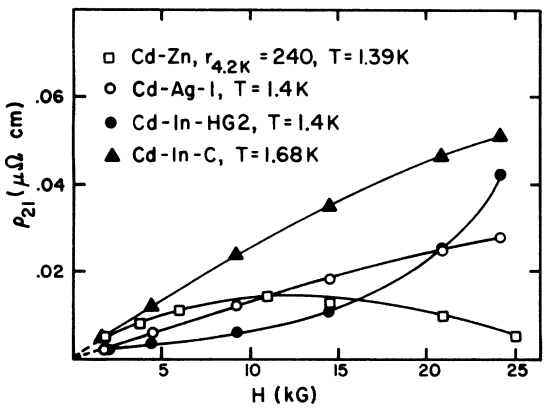

FIG. 6. Field dependence of ρ_{21} for some alloys (data for Cd-Zn taken from Ref. 1).

if intersheet scattering occurs in the present alloys, the values of $\omega\mathcal{T}$ ($T \to 0$) can be roughly estimated by comparing the behavior of $\rho_{21}(H)$ for the present alloys with that of sample *Cd*Zn 240 (Fig. 6). For sample Cd-In-*C*, with the curvature in $\rho_{21}(H)$ down, $\omega\mathcal{T} \leq 1$, while for sample Cd-In-*HG*2, with the curvature in $\rho_{21}(H)$ up, $\omega\mathcal{T} \geq 1$. But for both samples $\omega\tau$ ($T \to 0$) > 1 (and differ by a factor of 25), which rules out the constraint $\mathcal{T} \geq \tau$ in these alloys.

It is clear that no consistent behavior of ρ_{21} in terms of the intersheet scattering time $\mathcal{T}$ can be found. In terms of the theory an alteration of τ in a special manner can be considered. If the effect of the impurities is to alter τ so that $\omega\tau$ remains less than 1, the present data can qualitatively be understood. When $\omega\tau < 1$, intersheet scattering will not reverse the sign of ρ_{21}, since then the small-mass holes dominate the Hall resistivity[2] so that $\rho_{21} > 0$. Although the transverse magnetoresistance data[16] indicate that $\omega\tau \gg 1$ for these alloys in the field and temperature range considered, the possibility exists that the $\omega\tau$ appropriate for intersheet scattering in ρ_{21} (especially in the clover-leaf tip region) is different from the $\omega\tau$ in ρ_{11}. Perhaps neither is effectively measured by the zero-field conductivity. Such consideration would increase the number of unknown parameters in a meaningless manner. In the formalism the same τ was used to describe the normal scattering on all three bands; in the fit to the data $\omega\tau$ was shown to range from < 1 to $\gg 1$. To a high degree the success of the intersheet scattering, in its application to cadmium and the *Cd*Zn alloys from a simple model, rested on the parametrization of a single scattering time $\mathcal{T}$. The inclusion of more τ's as adjustable parameters into the intersheet formalism as it now stands would not gain any new ground. Any new results could just as easily be combined into the intersheet scattering time, which evidently would undergo redefinition with every sample. Such a formulation may be empirically useful, but it loses physical significance; it also would not remove the discontinuity in the approach to ρ_{21} of pure cadmium with decreasing impurity concentration. One is led by these arguments to conclude that intersheet scattering is inhibited by Ag or In at the level of a few ppm, and to look for a more flexible model to account for the experimental results.

B. Maximum near 5 K

The $\rho_{21}(T)$ curves for constant H depict for several samples a weak maximum at approximately 15 K and a pronounced maximum near 5 K. High-field ($\omega\tau \gg 1$) to low-field ($\omega\tau \ll 1$) transitions for electron (hole) orbits may be responsible for the low-temperature maximum. This idea has been used in the case of the noble metals[17] to account for the observed sharp rise in $|\rho_{21}(T)|$ with decreasing temperature for H parallel to a high-symmetry direction (such as [111]). It is assumed that with increasing temperature (decreasing τ) such transitions for hole orbits occur and reduce the number of hole states, N_h. Consequently $|\rho_{21}|$ decreases since, in a noncompensated metal for $\omega\tau \gg 1$, it is determined by $(N_h - N_e)^{-1}$.

It is true that the situation in a compensated metal is more complicated, but transitions from high- to low-field condition of hole (electron) orbits can be considered as an argument for a decrease (increase) in the positive value of the Hall resistivity. Here the observed initial increase of $\rho_{21}(T) > 0$ for T increasing from the residual temperature range could be the consequence of a reduction in electronlike orbits due to high-to-low $(\omega\tau)_e$ transitions, the holelike orbits unaffected. The observed decrease of $\rho_{21}(T)$ with still increasing temperature suggests, along these lines, an accompanying net loss of hole states in the high-field condition due to high-to-low $(\omega\tau)_h$ transitions.

It is clear that understanding the details of such a process requires precise knowledge of the τ values on each possible carrier orbit. While such knowledge is at best incomplete, there is direct experimental evidence that for a given change in temperature $(\omega\tau)_h$ and $(\omega\tau)_e$ may vary by quite different amounts, thereby changing markedly the relative scattering between hole and electron states. A recent determination[5] of the mean free paths (and, thereby, scattering times) for electrons (l_e) and holes (l_h) yielded the relation

$$l^{-1}(T) - l^{-1}(0) \approx \tau^{-1}(T) - \tau^{-1}(0) = A_n T^n , \qquad (1)$$

with $n = 3$ for holes on the second-zone hole surface and $n = 5$ for electrons on the third-zone lens. This temperature dependence was observed for $\vec{H} \parallel [0001]$ involving the same orbits that control ρ_{21}.

Direct substitution for τ_h and τ_e from (1) into the standard two-band formula[18] for the Hall resistivity in a compensated metal,

$$\rho_{21}(H, T) = (\omega_h\tau_h - \omega_e\tau_e)\rho_{11}(0, T) , \qquad (2)$$

can only be done with caution, since (2) applies for large $\omega\tau$ to compensated metals with spherical bands. The observation that the transverse magnetoresistance maintains a nearly quadratic field dependence up to high fields [observed by one of us (D. A. L.) for $H \leq 125$ kG in a sample for which $r_{4.2\ \mathrm{K}} = 3 \times 10^4$], suggests compensation to very large $\omega\tau$ values, indeed. The criterion for sphericity is closely satisfied in cadmium[19] for the third-zone electron surface, but not (especially near point K of the Brillouin zone) for the first- and second-zone hole surfaces. Since for $T \approx 5$ K, $(\omega\tau)_f \gtrsim 10$ for $H = 10$ kG and $\rho_{21} \propto H$ for $H \lesssim 10$ kG, some qualitative success[20] can be achieved by assuming the applicability of Eq. (2) in this field range.

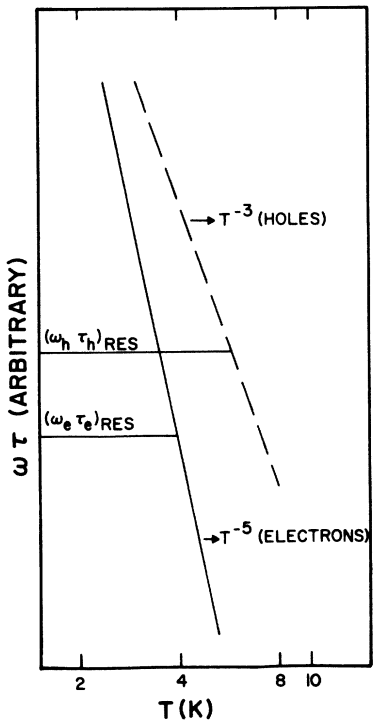

FIG. 7. Plot of $\omega\tau$ for holes and electrons assuming $\omega_h\tau_h > \omega_e\tau_e$ and different T dependence for τ.

One can then generate curves that exhibit a maximum in the observed temperature range for properly chosen coefficients A_n. The Hall resistivity remains positive when the residual values for $\omega_h\tau_h$ are chosen larger than the residual values $\omega_e\tau_e$, as illustrated in Fig. 7. A maximum occurs when the residual $\omega_h\tau_h$ is reached at a temperature higher than that where the residual $\omega_e\tau_e$ becomes the dominant quantity. Since the dependence of the residual value of $\omega_h\tau_h$ on impurity is not known, it is possible, as the results indicate, that the residual $\omega_h\tau_h$ increases faster with decreasing impurity content than the residual $\omega_e\tau_e$. When this relative position is reversed, ρ_{21} becomes negative at low temperatures.

A quantitative fit is difficult to achieve[21] for the combined T^3 and T^5 phonon scattering when reasonable values of A_n are chosen. An *ad hoc* separation of the problem into dominant electron scattering below the maximum and dominant hole scattering above the maximum yields a better fit.

Other experimental results[22] suggest considering anisotropies of scattering times varying with high powers of T. In these measurements on the radio-frequency size effect in cadmium, $l^{-1}(T)$ on the third-zone lens varied between T^3 and T^5 for $\vec{H}$ near [0001] and between T^6 and T^7 for $\vec{H}$ near $[10\bar{1}0]$. These data and those in Ref. 5 imply that the temperature dependence of $l^{-1}(T)$ and therefore $\tau^{-1}(T)$ could easily differ for several cyclotron orbits. Since all orbits contribute to the conductivity a restriction to two extreme orbits only can not be expected to give quantitative agreement with experimental results.

C. Closing remarks

The causes for the inhibition of the intersheet scattering remain undisclosed. However, several possibilities present themselves. A particular configuration of the solute atoms could produce locally a very small change in the contour of the Fermi sphere. At the clover-leaf tips, for instance, even a small change would have a large effect on the intersheet scattering parameter $\mathcal{T}$. Poorly soluble impurities can induce strain, and it is known that strain can have a large effect on small enclosed areas,[23] with a possible result in cadmium of large changes in $\mathcal{T}$. In fact, experiments under high pressure[24] indicate that the Fermi sphere seems to acquire the same topology as that of Zn. For this element the clover-leaf tips are joined and the problem of intersheet scattering is not present.

Without producing a traceable effect on the Fermi surface, impurities such as Ag or In that are not readily soluble in cadmium may induce defects, which, in combination with the impurities, or alone, could scatter carriers away from areas favorable for intersheet scattering.[25] In fact, recent diffusion data on Ag in cadmium[26] suggest that a decrease in overlapping defect ranges could very well be responsible for the critical onset of the intersheet scattering (and may account for the different magnitudes of $\rho_{21} < 0$ in the pure samples at low temperatures). Careful defect studies in cadmium with high-resolution x-ray diffractometry might shed more light on this.

Finally, if the low-temperature behavior of ρ_{21} in cadmium is indeed controlled by marked difference between $\tau_e(T)$ and $\tau_h(T)$, the effect of impurities may be simply to introduce large anisotropies in residual hole and electron scattering times (of which intersheet scattering can be considered as a special case). A variety of residual τ's for holes and electrons may lead to the residual Hall resistivities which are observed.

ACKNOWLEDGMENTS

The authors wish to thank Professor H. J. Yearian for orienting the single crystals and to thank Dr. R. T. Holm for the use of his Bridgman furnace. Financial assistance for the spectrographic sample analyses by an institutional grant from the Advanced Research Projects Agency and National Science Foundation is gratefully acknowledged. The high-field measurements were carried out with the assistance of Kurt Sohn.

† Work supported by a grant from the National Science Foundation.

‡This work is part of the dissertation by D. A. Lilly in partial fulfillment of the requirement for a Ph. D. degree.

*Present address: Aerospace Corporation, Bld. 120, Los Angeles, Calif. 90009.

[1]O. P. Katyal and A. N. Gerritsen, Phys. Rev. 178, 1037 (1969).

[2]Richard A. Young, J. Ruvalds, and L. M. Falicov, Phys. Rev. 178, 1043 (1969).

[3]H. Schwarz, Phys. Status Solidi 39, 515 (1970).

[4]D. A. Lilly and A. N. Gerritsen, in *Proceedings of the* 13th *International Low-Temperature Physics Conference*, Boulder, Colo. 1972, edited by R. H. Kropschot and K. D. Timmerhaus (University of Colorado Press, Boulder, Colorado, 1973).

[5]P. D. Hambourger, in Ref. 4.

[6]*The Art and Science of Growing Crystals*, edited by J. J. Gilman (Wiley, New York, 1963), p. 324.

[7]B. N. Aleksandrov, Zh. Eksp. Teor. Fiz. 43, 399 (1962) [Soviet Phys-JETP. 16, 286 (1963)].

[8]R. H. Bogaard and A. N. Gerritsen, Phys. Ref. B 3, 1808 (1971).

[9]*Constitution of Binary Alloys*, 2nd Suppl., edited by Francis Shunk (McGraw-Hill, New York, 1969), p. 215.

[10]*Constitution of Binary Alloys*, edited by Max Hansen (McGraw-Hill, New York, 1958), p. 14.

[11]Based on the crystal symmetry of cadmium, the resistivity tensor for $\vec{H} \| [0001]$ has the form

$$\begin{bmatrix} \rho_{11} & \rho_{12} & 0 \\ -\rho_{12} & \rho_{11} & 0 \\ 0 & 0 & \rho_{33} \end{bmatrix},$$

i.e., the resistivity is isotropic in the basal plane.

[12]J. R. Clement and E. H. Quinell, Rev. Sci. Instrum. 23, 213 (1952).

[13]P. H. Borcherds, Cryogenics 9, 138 (1969).

[14]D. C. Baird, *Experimentation: An Introduction to Measurement Theory and Experiment Design* (Prentice-Hall, New York, 1962), Chap. 3.

[15]R. W. Munn, Adv. Physics 18, 74 (1969).

[16]D. A. Lilly and A. N. Gerritsen, Physica 69, 286 (1973).

[17]C. M. Hurd and J. E. A. Alderson, J. Phys. Chem. Solids, 32, 175 (1970).

[18]A. H. Wilson, *The Theory of Metals*, (Cambridge U. P., New York, 1965), pp. 212–217; C. M. Hurd, *The Hall Effect in Metals and Alloys* (Plenum, New York, 1972), p. 90.

[19]R. W. Stark and L. M. Falicov, Phys. Rev. Lett. 19, 795 (1967).

[20]L. M. Falicov, A. B. Pippard, and Paul R. Sievert, Phys. Rev. 151, 498 (1966).

[21]D. A. Lilly, Ph. D. thesis (Purdue University, 1972) (unpublished).

[22]A. Myers, S. G. Porter, and R. S. Thompson, J. Phys. F 2, 24 (1972).

[23]A good example is the effect of strain on the basal plane needle contour in Be: L. R. Testardi and J. H. Condon, Phys. Rev. B 1, 3928 (1970).

[24]E. S. Itskevich and A. N. Vorooskii, Zh. Exsp. Teor. Fiz. Pis'ma Red. 4 226 (1966) [JETP Lett. 4, 154 1966].

[25]A. B. Pippard, Proc. R. Soc. A 287, 165 (1965).

[26]Chih-wen Mao, Phys. Rev. B 5, 4693 (1972).